JCTC Journal of Chemical Theory and Computation

Evaluation of B3LYP, X3LYP, and M06-Class Density Functionals for Predicting the Binding Energies of Neutral, Protonated, and Deprotonated Water Clusters

Vyacheslav S. Bryantsev,*,† Mamadou S. Diallo,† Adri C. T. van Duin,‡ and William A. Goddard III*,†

Materials and Process Simulation Center, Beckman Institute, MC 139-74, California Institute of Technology, Pasadena, California 91125, and Department of Mechanical and Nuclear Engineering, The Pennsylvania State University, University Park, Pennsylvania 16801

Received December 10, 2008

Abstract: In this paper we assess the accuracy of the B3LYP, X3LYP, and newly developed M06-L, M06-2X, and M06 functionals to predict the binding energies of neutral and charged water clusters including $(H_2O)_n$, $n = 2-8$, 20), $H_3O^+(H_2O)_n$, $n = 1-6$, and $OH^-(H_2O)_n$, $n = 1-6$. We also compare the predicted energies of two ion hydration and neutralization reactions on the basis of the calculated binding energies. In all cases, we use as benchmarks calculated binding energies of water clusters extrapolated to the complete basis set limit of the second-order Møller−Plesset perturbation theory with the effects of higher order correlation estimated at the coupled-cluster theory with single, double, and perturbative triple excitations in the aug-cc-pVDZ basis set. We rank the accuracy of the functionals on the basis of the mean unsigned error (MUE) between calculated benchmark and density functional theory energies. The corresponding MUE (kcal/mol) for each functional is listed in parentheses. We find that M06-L (0.73) and M06 (0.84) give the most accurate binding energies using very extended basis sets such as aug-cc-pV5Z. For more affordable basis sets, the best methods for predicting the binding energies of water clusters are M06-L/aug-cc-pVTZ (1.24), B3LYP/6-311++G(2d,2p) (1.29), and M06/aug-cc-PVTZ (1.33). M06-L/aug-cc-pVTZ also gives more accurate energies for the neutralization reactions (1.38), whereas B3LYP/6-311++G(2d,2p) gives more accurate energies for the ion hydration reactions (1.69).

1. Introduction

There is growing interest and need for describing various phenomena in inhomogeneous aqueous environments, for example, in the context of solvation of neutral and ionic solutes, ion complexation, solute transport, and partitioning at an organic liquid−water interface. Although the importance of polarization and charge transfer in inhomogeneous aqueous environments has been recognized,[1] it has been difficult to explicitly include them in a broadly applicable classical force field. Moreover, only a few empirical potential functions allow autoionization and charge migration.[2] The majority of theoretical studies of aqueous reactions reported thus far are based on the use of wave function methods and density functional theory (DFT).

The selection of the exchange-correlation functional in DFT is critical for correctly predicting the properties of aqueous systems.[3−5] Todorova et al.[3a] reported that hybrid functionals (B3LYP, X3LYP, PBE0) [modified with short-range Hartree−Fock exchange within a plane wave framework] give better results than generalized gradient approximation (GGA) functionals (BLYP, XLYP, and PBE) in

* Corresponding author phone: (626) 395-2730; fax: (626) 585-0918; e-mail: slava@wag.caltech.edu (V.S.B.), wag@wag.caltech.edu (W.A.G.).

† California Institute of Technology.

‡ The Pennsylvania State University.

10.1021/ct800549f CCC: $40.75
Published on Web 03/12/2009

reproducing the experimental structural (radial distribution function) and dynamical (self-diffusion constant) properties of liquid water. Tuckerman et al.[4] employed ab initio molecular dynamics simulations to probe the structure and transport mechanism of OH^-(aq) in water. They compared the performance of three DFT functionals: BLYP, PW91, and HCTC. They found that the BLYP functional reproduced the experimental findings that the diffusion of OH^-(aq) is slower than that of H^+(aq) and much faster than that of pure water. In contrast, the PW91 (HCTC) functional yields a OH^-(aq) diffusion that is too fast (slow) in comparison to a H^+(aq) diffusion.

McGrath et al.[5] showed that the computed thermodynamic properties of water (e.g., vapor−liquid coexistence curves) are sensitive not only to the density functional used, but also to the size of the basis set employed. PBE predicted a higher critical temperature and boiling point than experiment, while BLYP provided a better performance with small basis sets (double- and triple-ζ basis sets). These results were consistent with the ability of PBE and BLYP to describe the energetics of small water clusters. We have recently developed a computational methodology that gives accurate hydration free energies for ionic solutes.[6] This methodology, which couples DFT with mixed cluster/continuum models, is predicated upon the accurate calculations of the difference in total binding energies between relatively large ion−water clusters ($X^{m\pm}(H_2O)_n$) and pure water clusters ($(H_2O)_n$).[6] Thus, the correct description of water and solute−water clusters is critical for the accurate prediction of the thermodynamic properties of pure water and aqueous solutions.

Several reports devoted to the ability of DFT methods to describe hydrogen bonds in water clusters have appeared in the literature.[7−19] However, these previous studies have focused primarily on small neutral water clusters rarely containing more than six water molecules.[10,15,17] Only a few studies have tested the accuracy of DFT methods to predict the binding energies of $H_3O^+(H_2O)_n$ and $OH^-(H_2O)_n$ clusters.[19] Dahlke and Truhlar showed[13] that most of the hybrid functionals (which include Hartree−Fock exchange) gave more accurate binding energies and many-body components of the full interaction energy than the general-purpose GGA functionals. They also pointed out that these results are highly basis set dependent and that the choice of the appropriate basis set for each DFT method is very important for obtaining accurate results.[12,13] Santra et al.[16] examined the performance of density functionals in the limit of a complete basis set and found that the hybrid functionals (X3LYP and PBE0) gave binding energies for water clusters that were in closer agreement with benchmark binding energies calculated at the second-order Møller−Plesset (MP2)/complete basis set (CBS) level of theory. Similarly, Svozil et al.[15] reported improved results with the hybrid functionals (B3LYP and PBE0) for the description of the autoionization of a water octamer.

Zhao and Truhlar have recently developed the M06 family of local (M06-L) and hybrid (M06, M06-2X) meta-GGA functionals that show promising performance for noncovalent interactions.[20] This includes the binding energies in the two HB6/04 and JHB7 hydrogen-bonded databases. M06-L has been shown to provide accurate reaction energies for neutralization reactions involving small hydronium and hydroxide clusters.[19] In addition, M06-L and M06-2X have been tested to reproduce the relative energies of low-lying isomers of water hexamers.[18]

In this paper, we report a comparative study of the accuracy of the B3LYP[21] and X3LYP[22] functionals and the newly developed M06-L, M06-2X, and M06 functionals[20] to predict the binding energies of neutral ($(H_2O)_n$, $n = 2-8$, 20), protonated ($H_3O^+(H_2O)_n$, $n = 1-6$), and deprotonated ($OH^-(H_2O)_n$, $n = 1-6$) water clusters. B3LYP was selected given its widespread use, and X3LYP was included because of its excellent performance on small water clusters.[10,16] The accuracy of each method was evaluated using several basis sets. We also assessed the effect of basis set superposition error (BSSE) correction as calculated for the smallest basis set. As a benchmark for determining the accuracy of DFT functionals, we employed binding energies calculated at the complete basis set limit of the MP2 theory[23] with coupled-cluster theory with single, double, and perturbative triple excitations [CCSD(T)]/aug-cc-pVDZ corrections that were either compiled from the literature or calculated in this work.

2. Computational Methods

We used the second-order Möller−Plesset perturbation theory (MP2)[23] in the complete basis set (CBS) limit and coupled-cluster theory with singles, doubles, and perturbative triples excitations (CCSD(T))[24] in the aug-cc-pVDZ basis set[25] to determine the benchmark binding energies of hydrogen-bonded complexes against which the density functionals are evaluated. The effect of the basis set size (e.g., larger than aug-cc-pVDZ) on CCSD(T) corrections for water[26] and ion−water[27,28] clusters was shown to be relatively small (<0.2 kcal/mol). Thus, the combination of MP2/CBS with CCSD(T)/aug-cc-pVDZ corrections provides an excellent compromise between accuracy and computational cost and thus has been applied to water clusters as large as octamers.

For the basis set expansion in our MP2 calculations, we used a family of augmented correlation-consistent basis sets[25] (aug-cc-pVnZ, n = D, T, Q, 5). Only the valence electrons were correlated in the MP2 calculations. The largest basis set for geometry optimization was aug-cc-pVTZ. A test calculation for $OH^-(H_2O)$ reveals that the O−O distances differ by only 0.002 Å and the binding energies differ by <0.01 kcal/mol when compared to results obtained after full optimization at the MP2/aug-cc-pVQZ level. A BSSE-corrected intermolecular interaction energy (ΔE^b_e) was calculated with each basis set via the function counterpoise method[29] by taking into account the fragment relaxation energy terms resulting from the geometry change of the isolated fragments during the cluster formation:[30a]

$$\Delta E^b_e = E^{full}(\text{full}) - \sum_{fragm} E^{full}(\text{fragm}) + \sum_{fragm} \Delta E^{fragm}_{relax}(\text{fragm}) \quad (1)$$

where E^{full} and E^{fragm} are, respectively, the energies calculated with the full and fragment-only basis sets. Compared to the

method of Valiron and Mayer,[30b] which explicitly considers the hierarchy of *N*-body interactions for calculating the BSSE-corrected interaction energy, eq 1 does not include the three-body and higher many-body corrections. To estimate the MP2/CBS limit of the interaction energy, we utilized both the uncorrected and BSSE-corrected energies in an extrapolation scheme based on a polynomial function of inverse powers of 4 and 5:[31−33]

$$\Delta E(n) = \Delta E_{CBS} + B/(l_{max} + 1)^4 + C/(l_{max} + 1)^5 \quad (2)$$

where $n = 2$, 3, 4, and 5 for $n =$ D, T, Q, and 5 in aug-cc-pV*n*Z, respectively, and ΔE_{CBS}, B, and C are the fitting parameters.

We examined the ability of five density functionals [including two hybrid GGAs (B3LYP and X3LYP), one local meta-GGA (M06-L), and two hybrid meta-GGAs (M06-2X and M06)] to reproduce benchmark binding energies (MP2/CBS + ΔCCSD(T)) for a database of 27 pure, hydroxide, and hydronium water clusters. For each of these functionals, three different basis sets were considered: 6-311++G**, aug-cc-pVTZ, and aug-cc-pV5Z. For B3LYP, we also tested an empirically optimized 6-311++G(2d,2p) basis set. The small 6-311++G** basis set was selected as it provides reasonable dissociation energies for covalent bonds[34] and is computationally affordable for relatively large molecular systems. The geometries of all but $(H_2O)_{20}$ clusters were also optimized with the aug-cc-pVTZ basis set. $(H_2O)_{20}$ clusters were optimized using the aug-cc-pVDZ basis set followed by single-point energy calculations with the aug-cc-pVTZ basis set. Finally, single-point energy calculations for complexes containing up to five water molecules were performed using a very large aug-cc-pV5Z basis set. This basis set is sufficient to give converged DFT interaction energies for water clusters[12,16] and is expected to reflect a true performance of the tested functionals at the basis set limit. The BSSE correction in DFT methods is usually much smaller than in the explicitly correlated methods as MP2 and was investigated only for the smallest 6-311++G** basis set.[10,35] All MP2, CCSD(T), and DFT calculations were carried out using the NWChem 5.1 program package.[36] For the numerical integration grid in the DFT methods, the NWChem default grid was used for $(H_2O)_{20}$ in the aug-cc-pVTZ basis set and the ultrafine grid for the rest of the calculations. This corresponds to a target accuracy of 10^{-6} and 10^{-8} hartree, respectively.

3. Database of Accurate Water Cluster Binding Energies

The compiled database consists of 27 cluster binding energies extrapolated to the CBS limit of the MP2 and CCSD(T) theory. This includes a set of 14 neutral water clusters ($(H_2O)_n$, $n = 2-6,8,20$), 5 hydronium ion clusters ($H_3O^+(H_2O)_n$, $n = 1-3,6$), 7 hydroxide ion clusters ($OH^-(H_2O)_n$, $n = 1-6$), and 1 autoionized water cluster ($H_3O^+(H_2O)_4OH^-$). The structures of these clusters are shown in Figure 1, and the Cartesian coordinates (obtained after geometry optimization at the B3LYP/6-311++G(2d,2p) level of theory) are given in the Supporting Information.

Table 1. Total Water Binding Energies for $OH^-(H_2O)_n$ Clusters (kcal/mol)[a]

method	$OH^-(H_2O)$		$OH^-(H_2O)_2$		$OH^-(H_2O)_3$		$OH^-(H_2O)_4$ (C_s)		$OH^-(H_2O)_4$ (C_4)		$OH^-(H_2O)_5$		$OH^-(H_2O)_6$	
	$-\Delta E_e$	$-\Delta E^b_e$	$-\Delta E_e$	$-\Delta E^b_e$	$-\Delta E_e$	$-\Delta E^b_e$	$-\Delta E_e$	$-\Delta E^b_e$	$-\Delta E_e$	$-\Delta E^b_e$	$-\Delta E_e$	$-\Delta E^b_e$	$-\Delta E_e$	$-\Delta E^b_e$
MP2/aug-cc-pVDZ	26.73	24.68	48.65	45.13	68.07	62.82	85.86	78.40	85.86	78.63	101.95	92.65	117.96	106.26
MP2/aug-cc-pVTZ	27.17	25.85	49.12	47.04	68.22	65.30	86.04	81.85	85.61	81.67	101.87	96.69	117.52	111.12
MP2/aug-cc-pVQZ[b]	26.95	26.12	48.80	47.56	67.76	66.15	85.30	83.03	84.86	82.78	100.86	98.15	116.15	112.86
MP2/aug-cc-pV5Z[b]	26.71	26.27	48.49	47.81	67.36	66.50	84.72	83.51	84.32	83.22	100.16		115.33	
MP2/aug-cc-pV6Z[b]	26.62	26.36												
MP2/CBS (eq 2)	26.40	26.48	47.97	48.10	66.71	66.86	83.84	84.00	83.51	83.66	99.12	99.39	114.19	114.33
MP2/CBS best estimate[c]	26.44 ± 0.04		48.04 ± 0.06		66.79 ± 0.07		83.92 ± 0.08		83.58 ± 0.07		99.26 ± 0.13		114.26 ± 0.07	
MP2/CBS (ref 28)	26.4−26.5		47.8−48.2											
MP2/CBS + ΔCCSD(T)[d]	26.59		48.39		67.58		84.84		84.79		100.66		115.69	

[a] ΔE_e and ΔE^b_e are uncorrected and BSSE-corrected energies, respectively. [b] Single-point energies on MP2/aug-cc-pVTZ-optimized geometries. [c] Obtained as an average of the extrapolated CBS values of ΔE_e and ΔE^b_e. [d] CCSD(T) corrections are calculated using the aug-cc-pVDZ basis set.

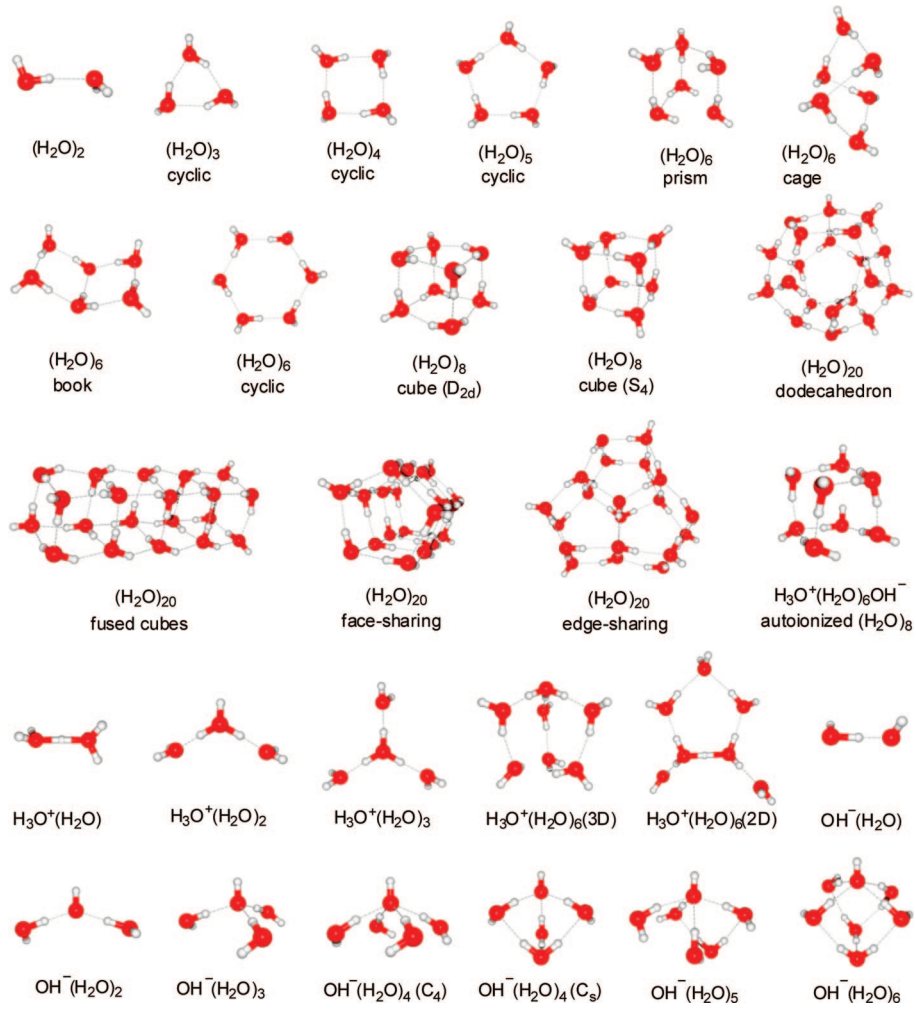

Figure 1. Structures of the studied pure, protonated, and deprotonated water complexes.

The structures and MP2/CBS binding energies of the neutral water clusters were taken from Xantheas and co-workers.[26,31−33] The reference binding energies of the lowest energy protonated water clusters $H_3O^+(H_2O)_{1-3}$ were computed in this study (see section 4.1). The estimated CCSD(T)/CBS interaction energies and the starting geometries of the two $H_3O^+(H_2O)_6$ isomers were taken from Shin et al.[37] (denoted as $2D_a$ and $3D_1$ in Figure 2 of ref 37). For the $OH^-(H_2O)_{1-6}$ clusters, the starting structures were based on the lowest energy conformers reported by Lee et al.[38] The results of high-level ab initio calculations for these systems are presented in section 4.1. The structure and relative energy of the autoionized water octamer [with respect to the S_4 cubic structure] at the MP2/CBS + ΔCCSD(T) level were taken from Svozil et al.[15] We expect the database of binding energies presented in this paper to have an accuracy of 0.5 kcal/mol or better and thus serve as a reliable benchmark for evaluating other methods.

4. Results and Discussion

4.1. Benchmark Binding Energies: MP2 and CCSD(T). The benchmark MP2 binding energies of the $OH^-(H_2O)_{1-6}$ and $H_3O^+(H_2O)_{1-3}$ clusters calculated with a series of correlation-consistent basis sets (aug-cc-pV*n*Z, n = D, T, Q, and 5) are shown in Tables 1 and 2, respectively. Figure 2 illustrates the effects of basis set size on the uncorrected and BSSE-corrected binding energies (ΔE_e and ΔE^b_e) for $OH^-(H_2O)$ and $H_3O^+(H_2O)$ complexes, respectively. A decrease of ΔE_e in going from the aug-cc-pVDZ to the aug-cc-pVTZ basis set is a typical feature of ion−water clusters,[30a] different from that for neutral water clusters.[31−33] However, such a minimum in ΔE_e for the aug-cc-pVTZ basis set becomes less pronounced with increasing size of a cluster and vanishes for $OH^-(H_2O)_{5-6}$.

The results in Tables 1 and 2 suggest that the magnitude of the BSSE correction decreases by 35−50% for each succeeding aug-cc-pV*n*Z set: For $OH^-(H_2O)$, for example, the BSSE correction is 2.05 (aug-cc-pVDZ), 1.33 (aug-cc-pVTZ), 0.83 (aug-cc-pVQZ), 0.44 (aug-cc-pV5Z), and 0.26 (aug-cc-pV6Z) kcal/mol. This trend points to a meaningful extrapolation toward a CBS limit, provided that sufficiently large basis sets are employed. We subsequently tested several extrapolation schemes based on exponential,[39] mixed exponential/Gaussian,[40] and inverse polynomial[31−33,41] functions. We found that a polynomial dependence of inverse powers of 4 and 5 (eq 2) gives the smallest difference of the extrapolated CBS values for the uncorrected and BSSE-corrected binding energies. This is the same CBS extrapolation scheme used by Xantheas and co-workers in their study of neutral water clusters.[31−33] The energies calculated with

Table 2. Total Water Binding Energies for $H_3O^+(H_2O)_n$ Clusters (kcal/mol)[a]

	$H_3O^+(H_2O)$		$H_3O^+(H_2O)_2$		$H_3O^+(H_2O)_3$	
method	$-\Delta E_e$	$-\Delta E^b_e$	$-\Delta E_e$	$-\Delta E^b_e$	$-\Delta E_e$	$-\Delta E^b_e$
MP2/aug-cc-pVDZ	34.05	31.77	57.81	54.35	77.82	73.13
MP2/aug-cc-pVTZ	34.55	33.29	58.13	56.43	77.97	75.68
MP2/aug-cc-pVQZ[b]	34.42	33.70	57.98	57.02	77.70	76.45
MP2/aug-cc-pV5Z[b]	34.27	33.91	57.75	57.28	77.40	76.77
MP2/CBS (eq 2)	34.00	34.18	57.33	57.58	76.89	77.13
MP2/CBS best estimate[c]	34.09 ± 0.09		57.46 ± 0.12		77.01 ± 0.12	
MP2/CBS (ref 27)	34.1−34.2		57.6−57.7			
MP2/CBS + ΔCCSD(T)[d]	33.53		56.85		76.46	

[a] ΔE_e and ΔE^b_e are uncorrected and BSSE-corrected energies, respectively. [b] Single-point energies at the MP2/aug-cc-pVTZ-optimized geometries. [c] Obtained as an average of the extrapolated CBS values of ΔE_e and ΔE^b_e. [d] CCSD(T) corrections are calculated using the aug-cc-pVDZ basis set.

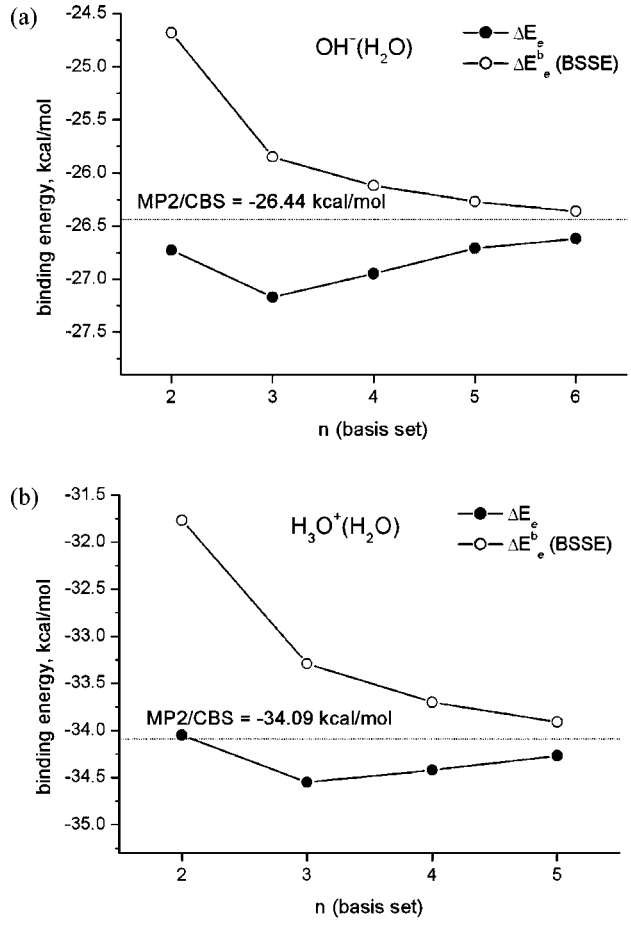

Figure 2. Variation in the MP2 binding energy for (a) $OH^-(H_2O)$ and (b) $H_3O^+(H_2O)$ with basis set size (aug-cc-pV*n*Z, $n = 2-6$), excluding (filled circles) and including (open circles) a BSSE correction. An extrapolated CBS limit is indicated as a horizontal line.

the aug-cc-pVDZ basis set were not included in the extrapolation, except for $OH^-(H_2O)_5$ and $OH^-(H_2O)_6$. The use of three consecutive BSSE-corrected energies for $OH^-(H_2O)_3$ and $OH^-(H_2O)_4$ clusters, with $n = 2-4$ and $n = 3-5$, yields CBS limit energies that are within 0.1 kcal/mol of each other. This gives us confidence that the extrapolation of results for $OH^-(H_2O)_5$ and $OH^-(H_2O)_6$ with only $n = 2-4$ energies available (aug-cc-pV*n*Z, $n =$ D, T, and Q) is reasonably accurate (within ~0.1 kcal/mol).

Our best estimates of the MP2/CBS values are obtained as an average of the extrapolated CBS values of ΔE_e and ΔE^b_e. The difference between these values is quite small and ranges from 0.08 kca/mol for $OH^-(H_2O)_5$ to 0.27 kcal/mol for $OH^-(H_2O)_5$. The results are given in Tables 1 and 2, together with previously reported MP2/CBS binding energies for $OH^-(H_2O)_{1-2}$ and $H_3O^+(H_2O)$.[27,28] Note that, in these previous studies,[27,28] geometry optimization was performed using a smaller aug-cc-pVDZ basis set and a different extrapolation scheme to reach the CBS limit was used. However, both computational protocols yielded very similar CBS values.

The effects of a higher order of electron correlation were examined using single-point CCSD(T)/aug-cc-pVDZ energy calculations at the MP2/aug-cc-pVDZ-optimized geometries. The results are listed in Tables 1−3. The inclusion of higher correlation at the CCSD(T) level decreases the binding energy of $H_3O^+(H_2O)_n$ by ~0.6 kcal/mol. The opposite effect is observed for $OH^-(H_2O)_n$. When the correlation effects are included at the CCSD(T) level, the binding energy progressively increases from ~0.2 kcal/mol for $OH^-(H_2O)$ to ~1.4 kcal/mol for $OH^-(H_2O)_6$. The magnitude of the average CCSD(T) correction for neutral water clusters is small (~0.18 kcal/mol). Overall, the results are variable, ranging from an increase of binding energy by ~0.1 kcal/mol for the $(H_2O)_6$ prism to a decrease in binding energy by ~0.5 kcal/mol for the $(H_2O)_6$ cyclic isomer. These results are consistent with a recent study of $(H_2O)_6$ isomers at the MP2 and CCSD(T) levels using the aug-cc-pVTZ basis set on oxygen and the cc-pVTZ basis set on hydrogen.[18]

4.2. A Comparative Study of the DFT Methods. The benchmark binding energies collected in the previous sections enable us to evaluate the performance of the DFT methods in reproducing the binding energies of neutral, protonated, and deprotonated water clusters. The discussion is organized as follows: We first consider the overall performance of 21 theoretical models resulting from a combination of 5 density functionals, several basis sets, and a set of BSSE-corrected results for our smallest basis set. Then we discuss the ability of DFT methods to accurately predict the relative stability of low-lying structural isomers and describe the binding energies of a series of large water clusters ($(H_2O)_{20}$ isomers). Finally, the density functionals are tested for their ability to reproduce the reaction energies of two ion hydration and neutralization reactions.

4.2.1. Overall Performance of the DFT Methods for an Accurate Database of MP2/CBS + ΔCCSD(T) Binding

Table 3. Comparison of the Benchmark Water Binding Energies (MP2/CBS + ΔCCSD(T)) to Those Obtained with Various DFT Methods (kcal/mol)[a]

	OBS[b]	aug-cc-pVTZ					aug-cc-pV5Z[c]					CBS	
complex	B3LYP	B3LYP	X3LYP	M06-L	M06-2X	M06	B3LYP	X3LYP	M06-L	M06-2X	M06	MP2	CCSD(T)
$(H_2O)_2$	4.97	4.57	4.95	4.74	5.17	4.79	4.55	4.93	4.70	5.09	4.73	4.98[e]	5.01
$(H_2O)_3$ cyclic	15.33	14.35	15.45	15.90	17.03	16.09	14.27	15.35	15.64	16.82	15.78	15.8[e]	15.8
$(H_2O)_4$ cyclic	27.42	26.05	27.76	27.22	28.76	27.33	25.84	27.52	26.69	28.43	26.82	27.6[e]	27.4
$(H_2O)_5$ cyclic	36.13	34.55	36.76	35.08	37.32	35.04	34.24	36.42	34.49	36.91	34.54	36.3[e]	35.9
$(H_2O)_6$ prism	44.03	41.14	44.33	47.31	50.04	47.82						45.9[e]	46.0
$(H_2O)_6$ cage	44.08	41.50	44.60	46.85	49.43	47.20						45.8[e]	45.8
$(H_2O)_6$ book	44.84	42.58	45.49	44.94	47.62	45.09						45.6[e]	45.3
$(H_2O)_6$ cyclic	44.63	42.81	45.51	43.08	46.11	43.36						44.8[e]	44.3
$(H_2O_8$ cube (D_{2d})	70.37	66.28	71.00	73.63	77.34	74.54						72.7[f]	72.6[h]
$(H_2O)_8$ cube (S_4)	70.34	66.24	70.96	73.62	77.34	74.52						72.7[f]	
$(H_2O)_{20}$ dodecahedron[d]	195.12	185.45	198.14	192.76	200.63	187.60						200.1[g]	
$(H_2O)_{20}$ fused cubes[d]	195.67	184.10	198.02	211.80	221.16	212.56						212.6[g]	
$(H_2O)_{20}$ face-sharing[d]	197.19	185.75	199.59	207.72	220.80	210.95						215.0[g]	
$(H_2O)_{20}$ edge-sharing[d]	199.97	188.85	202.56	206.03	223.71	209.16						217.9[g]	
$H_3O^+(H_2O)$	35.29	35.18	35.67	34.33	36.14	34.69	35.05	35.54	34.43	35.97	34.92	34.1	33.5
$H_3O^+(H_2O)_2$	58.64	58.37	59.35	57.14	59.92	57.05	58.18	59.16	57.10	59.61	57.15	57.5	56.9
$H_3O^+(H_2O)_3$	77.97	77.31	78.76	76.27	79.18	76.37	77.10	78.55	76.13	78.82	76.43	77.0	76.5
$H_3O^+(H_2O)_6$ (3*D*)	117.57	114.92	118.58	117.47	121.38	116.10						118.3[i]	117.8[i]
$H_3O^+(H_2O)_6$ (2*D*)	115.83	113.94	117.00	113.81	118.41	114.06						115.7[i]	114.9[i]
$OH^-(H_2O)$	29.01	27.43	27.97	27.29	30.11	27.55	26.92	27.45	26.07	29.39	26.93	26.4	26.6
$OH^-(H_2O)_2$	51.11	48.88	49.90	49.34	52.58	48.81	48.26	49.27	47.85	51.80	48.24	48.0	48.4
$OH^-(H_2O)_3$	69.89	66.88	68.37	70.22	73.29	69.82	66.20	67.67	68.50	72.53	69.07	66.8	67.6
$OH^-(H_2O)_4$ (C_4)	84.63	80.69	82.95	87.63	91.12	87.37	79.99	82.23	85.84	90.35	86.43	83.6	84.8
$OH^-(H_2O)_4$ (C_s)	85.45	81.33	83.83	87.74	91.84	87.25	80.60	83.07	85.73	90.87	86.23	83.9	84.8
$OH^-(H_2O)_5$	99.58	94.61	97.84	104.22	108.23	103.87	93.81	97.00	102.12	107.29	102.59	99.3	100.7
$OH^-(H_2O)_6$	114.32	108.57	112.55	119.19	123.78	119.01						114.3	115.7
$(H_2O)_8$ cube (S_4)−$H_3O^+(H_2O)_6OH^-$	24.42	22.94	23.26	29.64	23.45	30.91						25.3[j]	28.5[j]
MAE MP2, neutral	4.83	9.54	3.95	**2.57**	3.19	2.59							
MAE CCSD(T), neutral	0.83	2.70	0.82	**0.72**	2.30	0.87	1.29	**0.28**	0.64	0.79	0.56		
MAE CCSD(T), protonated	1.23	1.57	1.96	**0.54**	3.10	0.80	1.16	2.13	**0.49**	2.52	0.57		
MAE CCSD(T), deprotonated	**1.52**	3.26	1.79	2.44	6.06	2.16	2.96	1.64	**0.90**	4.90	1.15		
MAE CCSD(T), total	1.29	2.75	1.59	**1.24**	3.80	1.33	2.03	1.33	**0.73**	3.08	0.84		

[a] The lowest mean absolute error (MAE) for the two groups of basis sets is in bold. [b] Using the optimal 6-311++G(2d,2p) basis set (OBS) for B3LYP. [c] aug-cc-pV5Z single-point energies on aug-cc-pVTZ-optimized geometries. [d] aug-cc-pVTZ single-point energies on aug-cc-pVDZ-optimized geometries for the DFT methods. [e] Reference 31. [f] Reference 32. [g] Reference 33. [h] Reference 26. [i] Reference 37. [j] Reference 15.

Energies. Table 3 lists calculated binding energies of water clusters using the five DFT functionals with the 6-311++G(2d,2p) and aug-cc-pV*n*Z basis sets (n = T, 5). The DFT binding energies are compared with the benchmark estimates at the MP2/CBS and CCSD(T)/CBS levels. The MP2/CBS energies are given because they are considered to be reasonably accurate for neutral water clusters[31−33] and can also serve as a benchmark when CCSD(T) calculations are not feasible. DFT binding energies (both uncorrected and BSSE-corrected) calculated with the 6-311++G** basis set are included as Supporting Information (Table 1S). The accuracy of each method (density functional/basis set) is characterized by the mean unsigned error (MUE), averaged over the subset of neutral, protonated, and deprotonated clusters as well as the total data set. Note that the MUE for the largest aug-cc-pV5Z set may be biased since calculations with this basis set did not include clusters containing more than five water molecules.

The M06-L/aug-cc-pV5Z functional with an MUE of 0.73 kcal/mol shows the best overall performance. It gives the most accurate binding energies for $H_3O^+(H_2O)_n$ and $OH^-(H_2O)_n$ clusters. The M06/aug-cc-pV5Z functional with an MUE of 0.84 kcal/mol is the second best. X3LYP, B3LYP, and M06-2X [with the aug-cc-pV5Z basis set] are less accurate than M06-L by a factor of 1.8, 2.8, and 4.3, respectively. The overall accuracy of the M06-L and M06 potentials at the near CBS limit is impressive. However, from the practical point of view, the aug-cc-pV5Z basis set (287 basis functions per H_2O) is expensive even for medium-sized clusters.

If the largest aug-cc-pV5Z basis set is excluded, the best methods ranked by their mean unsigned error (kcal/mol, in parentheses) are M06-L/aug-cc-pVTZ (1.24), B3LYP/6-311++G(2d,2p) (1.29), and M06/aug-cc-pVTZ (1.33). The largest errors of M06-L/aug-cc-pVTZ and M06/aug-cc-pvTZ are due to the overbinding of $OH^-(H_2O)_n$ clusters (on average, by 2.2−2.4 kcal/mol). Interestingly, the DFT binding energy of $OH^-(H_2O)_n$ converges much more slowly with respect to basis set size than that of $(H_2O)_n$ and $H_3O^+(H_2O)_n$. For example, as one goes from the aug-cc-pVTZ to the aug-cc-pV5Z basis set, the M06-L binding energy decreases by 0.3, 0.1, and 1.7 kcal/mol for $(H_2O)_3$, $H_3O^+(H_2O)_3$, and $OH^-(H_2O)_3$, respectively. Thus, very large basis sets are needed for M06-L and M06 to accurately describe the energetics of different types of complexes.

As M06-L and M06 methods show the overall best performance at the basis set limit, this is not the case with the B3LYP functional. B3LYP/6-311++G** systematically overbinds, while B3LYP/aug-cc-pVTZ systematically underbinds, except for small ion−water clusters. On the basis of the performance for small water clusters, the 6-31+G(d,2p) basis set was recommended as an optimal basis set for B3LYP.[13] After testing several basis sets, we found that 6-311++G(2d,2p) provides a better and nearly optimal performance for the data set of binding energies employed in this study. B3LYP/6-311++G(2d,2p) has a mean unsigned error only 0.05 kcal/mol higher than that of M06-L/aug-cc-pVTZ and 0.04 kcal/mol lower than that of M06/aug-cc-pVTZ. However, the B3LYP/6-311++G(2d,2p) method is much more affordable than the M06 and M06-L methods since the 6-311++G(2d,2p) basis set employs approximately half Gaussian basis functions as the aug-cc-pVTZ basis set.

The X3LYP functional with the aug-cc-pV5Z basis set has the lowest MUE for the pure water clusters (0.28 kcal/mol). However, due to sizable errors for $H_3O^+(H_2O)_n$ and $OH^-(H_2O)_n$ clusters, X3LYP ranks fourth for overall performance (an MUE of 1.33 and 1.59 kcal/mol with the aug-cc-pV5Z and aug-cc-pVTZ basis sets, respectively). M06-2X does very poorly in almost each category, significantly overbinding even in the CBS limit, and particularly for $OH^-(H_2O)_n$ clusters. Its mean unsigned error is 3−4 times larger than the error obtained with the best DFT methods utilizing the same basis set (either aug-cc-pVTZ or aug-cc-pV5Z).

The utilization of a relatively small 6-311++G** basis set leads to significant overbinding for all the tested functionals (Table 1S of the Supporting Information). In this case, the mean unsigned errors sorted in increasing order are 4.2 (B3LYP), 5.9 (M06-L), 6.3 (X3LYP), 7.5 (M06), and 9.6 (M06-2X) kcal/mol. The inclusion of the BSSE correction (eq 1) partially compensates an overbinding effect associated with the 6-311++G** basis set, reducing the MUE by a factor of 1.8−3.3: 1.7 (B3LYP), 1.9 (X3LYP), 2.1 (M06-L), 3.1 (M06), and 5.1 (M06-2X) kcal/mol. B3LYP has the lowest error for both the uncorrected and BSSE-corrected binding energies calculated with this basis set.

4.2.2. Relative Stability of Conformational Isomers. The ability of DFT to describe the relative energies of the low-energy isomers is critical for the successful description of water in inhomogeneous environments at extreme conditions and under nanoscale confinement. Below, we compare the performance of B3LYP and M06-L as a test case to illustrate the distinctly different behavior between two classes of functionals. The first group consists of B3LYP and X3LYP functionals, whereas the second group consists of M06-L and M06 functionals. Note that the density functionals within each group behave very similarly.

We first consider the water hexamer isomers. Besides a cyclic structure, which is the most stable for clusters with three to five water molecules, $(H_2O)_6$ can adopt a variety of three-dimensional forms. CCSD(T) calculations yield the following energy ordering of the four hexamer structures: prism < book < cage < cyclic.[18,42] M06-L correctly predicts the energetic ordering of these isomers, but overestimates the energy spacing between them. For example, the energy difference between the cyclic and prism hexamers is 4.2 kcal/mol at the M06-L/aug-cc-pVTZ level, which is 2.5 kcal/mol larger than the benchmark value. In contrast, B3LYP predicts almost the reverse order of the relative stability of the four isomers, although with a much smaller range of energies (0.81 kcal/mol at the B3LYP/6-311++G(2d,2p) level). For a more thorough discussion, the reader is referred to a recent study focused exclusively on the performance of several DFT methods for a set of water hexamers.[18]

For protonated water clusters $H_3O^+(H_2O)_n$, the lowest energy conformers for n = 3−5 have noncyclic two-dimensional structures,[43] but the global minimum for n = 6 is a three-dimensional structure (without zero-point energy

Table 4. Ion Hydration (1−8) and Neutralization (9−32) Reactions Considered in This Study

1	$H_3O^+ + (H_2O)_2 = H_3O^+(H_2O)_2$	17	$H_3O^+(H_2O) + OH^-(H_2O)_4 = 7H_2O$
2	$H_3O^+ + (H_2O)_3 = H_3O^+(H_2O)_3$	18	$H_3O^+(H_2O)_3 + OH^-(H_2O)_3 = 8H_2O$
3	$H_3O^+ + (H_2O)_6 = H_3O^+(H_2O)_6$	19	$H_3O^+(H_2O)_2 + OH^-(H_2O)_4 = 8H_2O$
4	$OH^- + (H_2O)_2 = OH^-(H_2O)_2$	20	$H_3O^+(H_2O) + OH^-(H_2O)_5 = 8H_2O$
5	$OH^- + (H_2O)_3 = OH^-(H_2O)_3$	21	$H_3O^+(H_2O)_6 + OH^-(H_2O) = 9H_2O$
6	$OH^- + (H_2O)_4 = OH^-(H_2O)_4$	22	$H_3O^+(H_2O)_3 + OH^-(H_2O)_4 = 9H_2O$
7	$OH^- + (H_2O)_5 = OH^-(H_2O)_5$	23	$H_3O^+(H_2O)_2 + OH^-(H_2O)_5 = 9H_2O$
8	$OH^- + (H_2O)_6 = OH^-(H_2O)_6$	24	$H_3O^+(H_2O) + OH^-(H_2O)_6 = 9H_2O$
9	$H_3O^+(H_2O) + OH^-(H_2O) = 4H_2O$	25	$H_3O^+(H_2O)_6 + OH^-(H_2O)_2 = 10H_2O$
10	$H_3O^+(H_2O)_2 + OH^-(H_2O) = 5H_2O$	26	$H_3O^+(H_2O)_3 + OH^-(H_2O)_5 = 10H_2O$
11	$H_3O^+(H_2O) + OH^-(H_2O)_2 = 5H_2O$	27	$H_3O^+(H_2O)_2 + OH^-(H_2O)_6 = 10H_2O$
12	$H_3O^+(H_2O)_2 + OH^-(H_2O)_2 = 6H_2O$	28	$H_3O^+(H_2O)_6 + OH^-(H_2O)_3 = 11H_2O$
13	$H_3O^+(H_2O)_3 + OH^-(H_2O) = 6H_2O$	29	$H_3O^+(H_2O)_3 + OH^-(H_2O)_6 = 11H_2O$
14	$H_3O^+(H_2O) + OH^-(H_2O)_3 = 6H_2O$	30	$H_3O^+(H_2O)_6 + OH^-(H_2O)_4 = 12H_2O$
15	$H_3O^+(H_2O)_3 + OH^-(H_2O)_2 = 7H_2O$	31	$H_3O^+(H_2O)_6 + OH^-(H_2O)_5 = 13H_2O$
16	$H_3O^+(H_2O)_2 + OH^-(H_2O)_3 = 7H_2O$	32	$H_3O^+(H_2O)_6 + OH^-(H_2O)_6 = 14H_2O$

correction).[37] Although all DFT methods correctly predict a lower electronic energy for the 3*D* conformer of $H_3O^+(H_2O)_6$, the M06-class functionals provide a slightly more accurate prediction of the relative energy of the 2*D* conformer.

For deprotonated water clusters $OH^-(H_2O)_n$, the hypercoordinated structures with four oxygen neighbors are the most stable species for $n > 4$.[38,44] For $OH^-(H_2O)_4$, however, three-coordinate (C_s) and four-coordinate (C_4) structures are essentially isoenergetic at the MP2/CBS + ΔCCSD(T) level (the C_s isomer is more stable by only 0.05 kcal/mol). The M06-L method with either aug-cc-pVTZ or aug-cc-pV5Z basis set accurately reproduces the small difference in binding energies between these two conformations (within 0.1 kcal/mol). In contrast, B3LYP/6-311++G(2d,2p) overestimates the stability of the three-coordinate cluster by 0.8 kcal/mol. The overall results of our calculations suggest that the M06-L and M06 functionals do a better job than the B3LYP and X3LYP functionals in reproducing relative energetics of isomeric structures of small water clusters.

4.2.3. $(H_2O)_{20}$ Water Clusters. Accurate binding energies for the lowest lying isomers of the four families of stable $(H_2O)_{20}$ clusters were calculated by Fanourgakis et al.[33] at the MP2/CBS level of theory. These benchmark data are used to evaluate the performance of DFT methods for water clusters this large. The results summarized in Table 3 suggest that all DFT methods with optimal basis sets for small water clusters [(6-311++G(2d,2p) for B3LYP and aug-cc-pVTZ for X3LYP, M06-L, and M06] significantly underestimate the binding energies of the $(H_2O)_{20}$ clusters. The average error over the four isomers compared to the MP2/CBS binding energies is 6.3 (M06), 6.8 (M06-L), 11.8 (X3LYP), and 14.4 (B3LYP) kcal/mol. Note that M06-2X/aug-cc-pVTZ yields larger binding energies for $(H_2O)_{20}$ compared to the MP2/CBS values (the average error is 5.2 kcal/mol) due to significant overbinding for smaller water clusters (e.g., by 4.7 kcal/mol for $(H_2O)_8$).

B3LYP and X3LYP correctly predict the edge-sharing prism to be the lowest energy isomer and the face-sharing pentagonal prism to be the second lowest lying isomer. These functionals, however, do not reproduce a much lower stability of the dodecahedron arrangement with respect to the other three families. For example, the dodecahedron is 12.5 kcal/mol less stable than the fused cubes at the MP2/CBS level, whereas there is a very small energy separation between these isomers (<1.0 kcal/mol) at the B3LYP and X3LYP levels. The M06-L and M06 methods predict a high relative energy for the dodecahedral structure, but give the reverse order of stability for the three lowest energy families of minima compared to the MP2/CBS results. Thus, none of the studied DFT methods provide a completely satisfactory description of absolute and relative binding energies of $(H_2O)_{20}$.

4.2.4. Reaction Energies for Ion Hydration and Neutralization Reactions. We examined two types of reactions: ion hydration and neutralization reactions. In the first reaction, an ionic solute is hydrated by a cluster of *n* water molecules to form an ion−water cluster:

$$X^{\pm} + (H_2O)_n = X^{\pm}(H_2O)_n \qquad (3)$$

where $X^{\pm}$ is either H_3O^+ or OH^-. An improved methodology for the calculation of the solvation free energies of charge solutes based on reaction 3 has been recently described in ref 6. Due to the need to locate the low-energy isomers of relatively large solute−water clusters, this approach would benefit from the use of computationally efficient density functional theory. It is thus of interest to examine the accuracy of DFT methods for predicting the energy difference between ion−water clusters and the corresponding neutral water clusters.

Using the most stable isomers, as determined at the MP2/CBS + ΔCCSD(T) level, six reaction energies were calculated with the aug-cc-pV5Z basis set and eight reaction energies were calculated with the other basis sets (Table 4). The mean unsigned error of the reaction energies for all 21 DFT methods is given in Table 5. As expected from the best performance for clusterization energies, M06-L/aug-cc-pV5Z and M06/aug-cc-pV5Z are also the best two methods for reaction energetics (an MUE of 1.09 and 1.25 kcal/mol, respectively). However, these methods are very expensive and not applicable for clusters with more than 5−6 water molecules. The B3LYP/6-311++G(2d,2p) method is of the most practical interest, because it has the next lowest error for the ion hydration reactions (1.69 kcal/mol) and is computationally affordable for relatively large systems. Considerably more expensive M06/aug-cc-pVTZ and M06-L/aug-cc-pVTZ methods have an MUE that is 0.2−0.3 kcal/mol higher than that of B3LYP/6-311++G(2d,2p). Finally, we note that, due to a partial cancellation of systematic errors

Table 5. Mean Unsigned Error (kcal/mol) in Energies of Ion Hydration and Neutralization Reactions Calculated with Various DFT Methods[a]

method	ion hydration[b]	neutralization[c]
MP2/CBS	**0.90**	2.28
B3LYP/6-311++G**	2.53	9.30
B3LYP/6-311++G**(BSSE)	2.29	2.71
B3LYP/6-311++G(2d,2p)	**1.69**	**1.93**
B3LYP/aug-cc-pVTZ	2.12	3.25
B3LYP/aug-cc-pV5Z	2.04	2.49
X3LYP/6-311++G**	2.91	13.22
X3LYP/6-311++G**(BSSE)	2.25	4.54
X3LYP/aug-cc-pVTZ	2.10	2.76
X3LYP/aug-cc-pV5Z	2.07	2.84
M06-L/6-311++G**	3.21	8.82
M06-L/6-311++G**(BSSE)	2.16	2.11
M06-L/aug-cc-pVTZ	1.98	**1.38**
M06-L/aug-cc-pV5Z	**1.09**	**0.95**
M06-2X/6-311++G**	2.69	17.26
M06-2X/6-311++G**(BSSE)	3.44	8.89
M06-2X/aug-cc-pVTZ	3.64	7.33
M06-2X/aug-cc-pV5Z	3.64	5.55
M06/6-311++G**	6.07	13.51
M06/6-311++G**(BSSE)	2.21	5.44
M06/aug-cc-pVTZ	1.87	2.15
M06/aug-cc-pV5Z	**1.25**	**1.02**

[a] Using the most stable isomers at the MP2/CBS + ΔCCSD(T) level, namely, the 3*D* isomer for $H_3O^+(H_2O)_6$, the C_s isomer for $OH^-(H_2O)_4$, and the prism isomer for $(H_2O)_6$. The four lowest errors of each reaction are in bold. [b] Ion hydration reactions: $X^\pm(H_2O)_n = X^\pm + (H_2O)_n$, where $X^\pm = H_3O^+$ and OH^-. Six reaction energies calculated with the aug-cc-pV5Z basis set and eight reaction energies calculated with the other basis sets (Table 4). [c] Neutralization reactions: $H_3O^+(H_2O)_n + OH^-(H_2O)_m = (m + n + 2)H_2O$. Fifteen reaction energies calculated with the aug-cc-pV5Z basis set and 24 reaction energies calculated with the other basis sets (Table 4). The reference reaction energy (MP2/CBS + ΔCCSD(T)) for $H_3O^+ + OH^- = 2H_2O$ is 255.6 ± 0.2 kcal/mol.

in the binding energies of pure water and ion−water clusters,[6] some of the methods that perform poorly for predicting clusterization energies do better for predicting ion hydration energies.

A second reaction of interest is the neutralization of a hydronium ion cluster by a hydroxide ion cluster:

$$H_3O^+(H_2O)_n + OH^-(H_2O)_m = (m + n + 2)H_2O \quad (4)$$

We considered all possible neutralization reactions for the most stable isomers at the CCSD(T)/CBS level (Table 4). They include 15 reactions with the aug-cc-pV5Z basis set and 24 reactions with the smaller basis sets. Table 5 lists the mean unsigned errors of the reaction energies for all 21 methods. Since there is no cancellation of systematic errors in neutralization reactions, the MUE in the reaction energies of this type of reaction is higher than that of ion hydration reactions in most cases. The only methods showing improved performance are M06 and M06-L with the largest aug-cc-pV5Z basis set (an MUE of 0.95−1.02 kcal/mol) and M06-L/aug-cc-pVTZ (an MUE of 1.38 kcal/mol). These are also the best two methods for describing neutralization reactions. In addition, Table 3 shows that M06-L/aug-cc-pvTZ is more accurate than other methods in predicting the energetics of the autoionization of a water octamer cluster ($H_3O^+(H_2O)_6OH^-$).[15] The overall results of our calculations support a conclusion recently drawn from a subset of smaller ion−water clusters[19] that M06-L/aug-cc-pVTZ gives accurate energies for neutralization reactions. B3LYP/6-311++G(2d,2p) has the fourth lowest MUE (1.93 kcal/mol), which is 0.22 kcal/mol lower than that of M06/aug-cc-pVTZ. Finally, we note that although MP2/CBS yields the smallest average error for ion hydration reactions (0.90 kcal/mol), this method is outperformed by the M06-L, B3LYP, and M06 functionals for neutralization reactions (2.28 kcal/mol).

5. Conclusions

We evaluated the ability of five density functionals [including two hybrid GGAs (B3LYP, X3LYP), one local meta-GGA (M06-L), and two hybrid meta-GGAs (M06-2X, M06) with several basis sets] to reproduce accurate binding energies of 27 neutral ($(H_2O)_n$, $n = 2-8$, 20), protonated ($H_3O^+(H_2O)_n$, $n = 1-6$), and deprotonated ($OH^-(H_2O)_n$, $n = 1-6$) water clusters. As a benchmark for determining the accuracy of the DFT method, we used binding energies extrapolated to the complete basis set limit of the MP2 theory with the effects of higher order correlation estimated at the CCSD(T)/aug-cc-pVDZ level. We established the CBS limit of the MP2 and CCSD(T) theory for a series of $OH^-(H_2O)_n$ ($n = 1-6$) and $H_3O^+(H_2O)_n$ ($n = 1-3$) clusters. We subsequently combined our estimates with CBS limit estimates taken from the literature to generate a database of highly accurate binding energies of water clusters that were used as benchmarks to compare the accuracy of the DFT functionals.

The M06-L and M06 functionals coupled with a very large aug-cc-pV5Z basis set show the best overall performance (a mean unsigned error of 0.73−0.84 kcal/mol). However, these methods are very expensive and therefore cannot be routinely used even for medium-sized clusters. If the aug-cc-pV5Z basis set is excluded, the best methods ranked by their mean unsigned error (kcal/mol, in parentheses) are M06-L/aug-cc-pVTZ (1.24), B3LYP/6-311++G(2d,2p) (1.29), M06/aug-cc-PVTZ (1.33), and X3LYP/aug-cc-pVTZ (1.59). The performance of M06-2X is relatively poor. M06-2X/aug-cc-pVTZ has an average error that is 3 times as large as those of the best methods.

The utilization of a relatively small 6-311++G** basis set leads to significant overbinding for all the tested functionals. This effect can be partially compensated by including the BSSE correction. B3LYP has the lowest average error for both the uncorrected and BSSE-corrected binding energies calculated with this basis set.

M06-L and M06 do a good job in reproducing the relative energetics of small clusters. However, none of the functionals gave adequate binding energies for the $(H_2O)_{20}$ clusters. The M06-L, M06, B3LYP, and X3LP methods with their optimal basis sets for small clusters underestimate binding energies for the four lowest lying isomers of stable $(H_2O)_{20}$ clusters.

M06-L and M06 functionals in the CBS limit are the most accurate methods for predicting reaction energetics. M06-L/aug-cc-pVTZ and B3LYP/6-311++G(2d,2p) are the best among the more cost-effective methods. M06-L/aug-cc-

pVTZ shows exceptional performance for neutralization reactions, whereas B3LYP/6-311++G(2d,2p) is more accurate for ion hydration reactions.

Acknowledgment. We are grateful to Dr. George S. Fanourgakis, Dr. Daniel Svozil, and Dr. P. Tarakeshwar for providing us with the Cartesian coordinates of $(H_2O)_{20}$, $H_3O^+(H_2O)_6OH^-$, and $OH^-(H_2O)_{5-6}$ clusters, respectively. This work was performed in part using the Molecular Science Computing Facility (MSCF) in the William R. Wiley Environmental Sciences Laboratory, a national scientific user facility sponsored by the U.S. Department of Energy's Office of Biological and Environmental Research located at the Pacific Northwest National Laboratory, which is operated for the Department of Energy by Battelle.

Supporting Information Available: Cartesian coordinates and energies for optimized clusters at the B3LYP/6-311++G(2d,2p) level of theory and Table 1S comparing the performance of the various DFT methods employing the 6-311++G** basis set. This material is available free of charge via the Internet at http://pubs.acs.org.

References

(1) (a) Mucha, M.; Frigato, T.; Levering, L. M.; Allen, H. C.; Tobias, D. J.; Dang, L. X.; Jungwirth, P. *J. Phys. Chem. B* **2005**, *109*, 7617–7623. (b) Vacha, R.; Buch, V.; Milet, A.; Devlin, J. P.; Jungwirth, P. *Phys. Chem. Chem. Phys.* **2005**, *7* (9), 4736–4747. (c) Wick, C. D.; Kuo, I.-F. W.; Mundy, C. J.; Dang, L. X. *J. Chem. Theory Comput.* **2007**, *3*, 2002–2010. (d) Jorgensen, W. L. *J. Chem. Theory Comput.* **2007**, *3*, 1877–1877. (e) Xie, W.; Gao, J. *J. Chem. Theory Comput.* **2007**, *3*, 1890–1900.

(2) (a) Stillinger, F. H.; David, C. W. *J. Chem. Phys.* **1978**, *69*, 1473–1484. (b) David, C. W. *J. Chem. Phys.* **1996**, *104*, 7255–7260. (c) Halley, J. W.; Rustad, J. R.; Rahman, A. *J. Chem. Phys.* **1993**, *98*, 4110–4119. (d) Corrales, L. R. *J. Chem. Phys.* **1999**, *110*, 9071–9080. (e) Lussetti, E.; Pastore, G.; Smatgiassi, E. *Chem. Phys. Lett.* **2003**, *381*, 287–291. (f) Garofalini, S. H.; Mahadevan, T. S. *J. Phys. Chem. B* **2007**, *111*, 8919–8927. (g) Goddard, W. A., III; Merinov, B.; van Duin, A. C. T.; Jacob, T.; Blanco, M.; Molinero, V.; Jang, S. S. *Mol. Simul.* **2006**, *32*, 251–268.

(3) (a) Todorova, T.; Seitsonen, A. P.; Hutter, J.; Kuo, I.-F. W.; Mundy, C. J. *J. Phys. Chem. B* **2006**, *110*, 3685–3691. (b) VandeVondele, J.; Mohamed, F.; Krack, M.; Hutter, J.; Sprik, M.; Parrinello, M. *J. Chem. Phys.* **2005**, *122*, 014515−1-6.

(4) (a) Tuckerman, M. E.; Marx, D.; Parrinello, M. *Nature* **2002**, *417*, 925–929. (b) Tuckerman, M. E.; Chandra, A.; Marx, D. *Acc. Chem. Res.* **2006**, *39*, 151–158.

(5) McGrath, M. J.; Siepmann, J. I.; Kuo, I.-F. W.; Mundy, C. *J. Mol. Phys.* **2006**, *104*, 3619–3626.

(6) Bryantsev, V. S.; Diallo, M. S.; Goddard, W. A., III. *J. Phys. Chem. B* **2008**, *112*, 9709–9719.

(7) Xantheas, S. S. *J. Chem. Phys.* **1994**, *102*, 4505–4517.

(8) Hall, R. J.; Hillier, I. H.; Vincent, M. A. *Chem. Phys. Lett.* **2000**, *320*, 139–143.

(9) Xu, X.; Goddard, W. A., III. *J. Phys. Chem. A* **2004**, *108*, 2305–2313.

(10) Su, J. T.; Xu, X.; Goddard, W. A., III. *J. Phys. Chem. A* **2004**, *108*, 10518–10526.

(11) Dahlke, E. E.; Truhlar, D. G. *J. Phys. Chem. B* **2005**, *109*, 15677–15683.

(12) Csonka, G. I.; Ruzsinszky, A.; Perdew, J. P. *J. Phys. Chem. B* **2005**, *109*, 21471–21475.

(13) Dahlke, E. E.; Truhlar, D. G. *J. Phys. Chem. B* **2006**, *110*, 10595–10601.

(14) Anderson, J. A.; Tschumper, G. S. *J. Phys. Chem. A* **2006**, *110*, 7268–7271.

(15) Svozil, D.; Jungwirth, P. *J. Phys. Chem. A* **2006**, *110*, 9194–9199.

(16) Santra, B.; Michaelides, A.; Scheffler, M. *J. Chem. Phys.* **2007**, *127*, 1–9.

(17) Shields, G. C.; Kirschner, K. N. *Synth. React. Inorg., Met.-Org., Nano-Met. Chem.* **2008**, *38*, 32–39.

(18) Dahlke, E. E.; Olson, R. M.; Leverentz, H. R.; Truhlar, D. G. *J. Phys. Chem. A* **2008**, *112*, 3976–3984.

(19) Dahlke, E. E.; Orthmeyer, M. A.; Truhlar, D. G. *J. Phys. Chem. B* **2008**, *112*, 2372–2381.

(20) (a) Zhao, Y.; Truhlar, D. G. *J. Chem. Phys.* **2006**, *125*, 1–17, 194101. (b) Zhao, Y.; Truhlar, D. G. *Theor. Chem. Acc.* **2008**, *120*, 215–241.

(21) (a) Becke, A. D. *Phys. Rev. A* **1988**, *38*, 3098–3100. (b) Lee, C. T.; Yang, W. T.; Parr, R. G. *Phys. Rev. B* **1988**, *37*, 785–789.

(22) Xu, X.; Goddard, W. A., III. *Proc. Natl. Acad. Sci. U.S.A.* **2004**, *101*, 2673–2677.

(23) Möller, C.; Plesset, M. S. *Phys. Rev.* **1934**, *46*, 618–622.

(24) (a) Purvis, G. D., III; Bartlett, R. J. *J. Chem. Phys.* **1982**, *76*, 1910–1918. (b) Raghavachari, K.; Trucks, G. W.; Pople, J. A.; Head-Gordon, M. *Chem. Phys. Lett.* **1989**, *157*, 479–483. (c) Watts, J. D.; Gauss, J.; Bartlett, R. J. *J. Chem. Phys.* **1993**, *98*, 8718–8733.

(25) (a) Dunning, T. H., Jr. *J. Chem. Phys.* **1989**, *90*, 1007–1023. (b) Kendall, R. A.; Dunning, T. H., Jr.; Harrison, R. J. *J. Chem. Phys.* **1992**, *96*, 6796–6806.

(26) Xantheas, S. S. *Struct. Bonding (Berlin)* **2005**, *116*, 119–148.

(27) Masamura, M. *Theor. Chem. Acc.* **2001**, *106*, 301–313.

(28) Masamura, M. *Int. J. Quantum Chem.* **2004**, *100*, 28–40.

(29) Boys, S. F.; Bernardi, F. *Mol. Phys.* **1970**, *19*, 553–566.

(30) (a) Xantheas, S. S. *J. Chem. Phys.* **1996**, *104*, 8821–8824. (b) Valiron, P.; Mayer, I. *Chem. Phys. Lett.* **1997**, *275*, 46–55.

(31) Xantheas, S. S.; Burnham, C. J.; Harrison, R. I. *J. Chem. Phys.* **2002**, *116*, 1493–1499.

(32) Xantheas, S. S.; Aprà, E. *J. Chem. Phys.* **2004**, *120*, 823–828.

(33) Fanourgakis, G. S.; Aprà, E.; Xantheas, S. S. *J. Chem. Phys.* **2004**, *121*, 2655–2663.

(34) Bryantsev, V. S.; Diallo, M. S.; Goddard, W. A., III. *J. Phys. Chem. A* **2007**, *111*, 4422–4430.

(35) Zhao, Y.; Truhlar, D. G. *J. Chem. Theory Comput.* **2005**, *1*, 415–432.

(36) Bylaska, E. J.; de Jong, W. A.; Govind, N.; Kowalski, K.; Straatsma, T. P.; Valiev, M.; Wang, D.; Apra, E.; Windus, T. L.; Hammond, J.; Nichols, P.; Hirata, S.; Hackler, M. T.; Zhao, Y.; Fan, P.-D.; Harrison, R. J.; Dupuis, M.; Smith,

D. M. A.; Nieplocha, J.; Tipparaju, V.; Krishnan, M.; Wu, Q.; Van Voorhis, T.; Auer, A. A.; Nooijen, M.; Brown, E.; Cisneros, G.; Fann, G. I.; Fruchtl, H.; Garza, J.; Hirao, K.; Kendall, R.; Nichols, J. A.; Tsemekhman, K.; Wolinski, K.; Anchell, J.; Bernholdt, D.; Borowski, P.; Clark, T.; Clerc, D.; Dachsel, H.; Deegan, M.; Dyall, K.; Elwood, D.; Glendening, E.; Gutowski, M.; Hess, A.; Jaffe, J.; Johnson, B.; Ju, J.; Kobayashi, R.; Kutteh, R.; Lin, Z.; Littlefield, R.; Long, X.; Meng, B.; Nakajima, T.; Niu, S.; Pollack, L.; Rosing, M.; Sandrone, G.; Stave, M.; Taylor, H.; Thomas, G.; van Lenthe, J.; Wong A.; Zhang, Z. *NWChem, A Computational Chemistry Package for Parallel Computers*, version 5.1; Pacific Northwest National Laboratory: Richland, WA, 2007.

(37) Shin, I.; Park, M.; Min, S. K.; Lee, E. C.; Suh, S. B.; Kim, K. S. *J. Chem. Phys.* **2006**, *125*, 1–7, 234305].

(38) Lee, H. M.; Tarkeshwar, P.; Kim, K. S. *J. Chem. Phys.* **2004**, *121*, 4657–4664.

(39) Feller, D. J. *J. Chem. Phys.* **1992**, *96*, 6104–6114.

(40) Peterson, K. A.; Wood, D. E.; Dunning, T. H., Jr. *J. Chem. Phys.* **1994**, *100*, 7410–7415.

(41) (a) Helgaker, T.; Klopper, W.; Koch, H.; Noga, J. *J. Chem. Phys.* **1997**, *106*, 9639–9646. (b) Halkier, A.; Helgaker, T.; Jorgensen, P.; Klopper, W.; Koch, H.; Olson, J.; Wilson, A. K. *Chem. Phys. Lett.* **1998**, *286*, 243–252.

(42) Dahlke, E. E.; Leverentz, H. R.; Truhlar, D. G. *J. Chem. Theory Comput.* **2008**, *4*, 33–41.

(43) (a) Jiang, J. C.; Wang, Y. S.; Chang, H. C.; Lin, S. H.; Lee, Y. T.; Niedner-Schatteburgm, G.; Chang, H. C. *J. Am. Chem. Soc.* **2000**, *122*, 1398–1410. (b) Lee, H. M.; Tarakeshwar, P.; Park, J. W.; Kolaski, M. R.; Yoon, Y. J.; Yi, H.-B.; Kim, W. Y.; Kim, K. S. *J. Phys. Chem. A* **2004**, *108*, 2949–2958. (c) Park, M.; Shin, I.; Singh, N. J.; Kim, K. S. *J. Phys. Chem. A* **2007**, *111*, 10692–10702.

(44) Masamura, M. *J. Comput. Chem.* **2001**, *22*, 31–37.

(45) (a) Li, X.; Teige, V. E.; Iyengar, S. S. *J. Phys. Chem. A* **2007**, *111*, 4815–4820. (b) Śmiechowski, M.; Stangret, J. *J. Phys. Chem. A* **2007**, *111*, 2889–2897. (c) Cappa, C. D.; Smith, J. D.; Messer, B. M.; Cohen, R. C.; Saykally, *J. Phys. Chem. A* **2007**, *111*, 4776–4785.

CT800549F